Published in final edited form as:
Bone. 2007 November ; 41(5): 752–759.

Mechanical Regulation of PTHrP Expression in Entheses

Xuesong Chen[1], **Carolyn Macica**[1], **Ali Nasiri**[1], **Stefan Judex**[2], and **Arthur E. Broadus**[1*]

1*Section of Endocrinology, Department of Internal Medicine, Yale University School of Medicine, New Haven, CT.*

2*Department of Biomedical Engineering, SUNY Stony Brook, Stony Brook, NY*

Abstract

The PTHrP gene is expressed in the periosteum and in tendon and ligament insertion sites in a PTHrP-lacZ knockin reporter mouse. Here, we present a more detailed histological evaluation of PTHrP expression in these sites and study the effects of mechanical force on PTHrP expression in selected sites. We studied the periosteum and selected entheses by histological, histochemical, and in situ hybridization histochemical techniques, and tendons or ligaments were unloaded by tail suspension or surgical transection. In the periosteum, PTHrP is expressed in the fibrous layer and the type 1 PTH/PTHrP receptor (PTH1R) in the subjacent cambial layer. PTHrP has distinct temporospatial patterns of expression in the periosteum, one hot spot being the metaphyseal periosteum in growing animals. PTHrP is also strongly expressed in a number of fibrous insertion sites. In the tibia these include the insertions of the medial collateral ligament (MCL) and the semimembraneosus (SM). In young animals, the MCL and SM sites display a combination of underlying osteoblastic and osteoclastic activities that may be associated with the migration of these entheses during linear growth. Unloading the MCL and SM by tail suspension or surgical transection leads to a marked decrease in PTHrP/lacZ expression and a rapid disappearance of the subjacent osteoblastic population. We have not been able to identify PTHrP-lacZ in any internal bone cell population in the PTHrP-lacZ knockin mouse in either a CD-1 or C57Bl/6 genetic background.

In conclusion, we have identified PTHrP expression in surface structures that connect skeletal elements to each other and to surrounding muscle but not in intrinsic internal bone cell populations. In these surface sites, mechanical force seems to be an important regulator of PTHrP expression. In selected sites and/or at specific times, PTHrP may influence the recruitment and/or activities of underlying bone cell populations.

Keywords

PTHrP; periosteum; enthesis; tendon and ligament insertion sites; mechanical loading

INTRODUCTION

The PTH and PTHrP genes are members of a small gene family [1–3]. What remains from this heritage is a similar structural organization of the two genes and a stretch of homologous

*Correspondence: Arthur E. Broadus, Section of Endocrinology, Department of Internal Medicine, Yale University School of Medicine, The Anlyan Center S-123, PO Box 208020, New Haven, CT 06520-8020, Tel 203-785-3966, Fax 203-737-4360, E-mail: arthur.broadus@yale.edu.

sequence at the N-terminus of each mature gene product. These N-terminal products appear to be served by a common receptor (the type 1 PTH/PTHrP receptor, PTH1R), although they function in two quite separate domains, PTH as a classical systemic peptide hormone and PTHrP as predominately an autocrine/paracrine regulatory molecule [1–5]. The segregation and specificity of PTH and PTHrP signaling in these two domains are more or less complete, and this is attributed to the lability and sequestration of PTHrP in its microenvironments as well as variations in PTH1R density in PTH and PTHrP targets [1,2,5–10].

As is common for many products that act locally, PTHrP is regulated primarily at the level of mRNA expression and is subject to very tight control [11]. One consequence of this tight regulation is a steady-state level of PTHrP mRNA in the 0.001% range (1 part in 100,000) [12], and this low-abundance has made it difficult in many sites to detect PTHrP mRNA and protein by conventional localization techniques of immunohistochemistry (IH) and in situ hybridization histochemistry (ISHH) [reviewed in 13]. For this reason, we recently created an allelic PTHrP-lacZ knockin mouse, in which β gal activity provides an approximately 5-fold increase in sensitivity as compared to IH and ISHH [13]. This mouse has provided a useful detection system, reliably reflecting known sites of PTHrP expression and identifying a number of sites that were previously unrecognized. Among the latter are the periosteum and tendon and ligament insertion sites (entheses) into cortical bone [13].

We report here additional findings regarding lacZ/PTHrP expression in the periosteum and selected entheses, using histological, histochemical, and ISHH techniques. We have also examined the effects of mechanical unloading on PTHrP expression in selected entheses.

MATERIALS AND METHODS

Animals and Procedures

The PTHrP-lacZ knockin mouse has been outbred onto a CD-1 background for routine use [13]. We have also inbred the PTHrP-lacZ allele onto a C57BL/6J background for nine generations, the incipient-congenic stage by Jackson Laboratory criteria. Mice were genotyped by PCR of tail DNA using lacZ coding-region primers [13]. We approached unloading of selected entheses using tail suspension or surgical transection of the tendon or ligament in question. The t½ of β-galactosidase (β gal) has been reported in the literature as 8, 13 and 43 hrs, for a mean of about 24 hr [14–16]. Using this figure, one would achieve ⅛ of an initial signal at 72 hrs (assuming complete shut down), so that this was chosen as our initial minimum period of post-manipulation observation with each technique. To our knowledge, there has been only one report of an unloaded enthesis, this being the tibial patellar insertion in rats sent into space in 1994; in this report there was pronounced cortical resorption at this site [17].

Tail suspension is regarded by NASA as the gold-standard for unloading the endosteal skeleton [18]. The initial experiments were performed at Stony Brook [19] and subsequent experiments in New Haven; in combination we unloaded about 40 PTHrP-lacZ mice of different ages and genders for periods ranging from 3 to 30 days (as compared to approximately 30 sham-unloaded controls). We settled upon mixed-gender PTHrP-lacZ mice at 5–7 weeks of age suspended for 11 days and describe the findings from 13 such mice in the text. We could not distinguish between the sexes in terms of responsiveness and have considered the findings together.

Surgical transection of the tendon/ligament immediately proximal to its insertion proved to be straightforward in sites that could be easily exposed. Here, we will focus on results at the middle collateral ligament (MCL), semimembranosus (SM), and semitendinosus (ST) entheses, which insert into a relatively small area on the proximal medial metaphysis of the tibia. Transection of these structures was virtually bloodless, and the entheses themselves were completely

untouched. Again, we piloted various ages and post-operative periods of observation and from these settled upon 5-week-old mice, which were sacrificed 7 days post-operatively. We studied 15 such mixed-gender PTHrP-lacZ mice using the unoperated side as control and usually splinting the operated knee with a loosely-fitting section of a drinking straw.

Specimens, sectioning, and staining

Bone specimens were rapidly dissected, with care taken to avoid damaging the surfaces, and were prefixed in 4% paraformaldehyde (PFA) for 1–2 hr on ice. A modification that has virtually eliminated endogenous β-gal activity in control tissues was to heat-inactive endogenous galactosidase activity in specimens by incubating them at 49°C for 10–15 min in PBS before X-gal staining [20]. Specimens were then incubated overnight at 37°C in the dark in 0.1% X-gal reaction buffer at pH 7.5, rinsed in PBS, and postfixed in 4% PFA overnight at 4°C [13]. Selected specimens were partially "cleared" after X-gal staining by digestion in 1% trypsin at 37°C for 24–72 hrs (based on age), washing in PBS, and then placing the specimen in 1% KOH for 1–2 weeks with fresh KOH every 2 days; the cleared samples were then stored in 70% ethanol. These were photographed under a dissecting microscope and are referred to in the text as cleared images.

Embedding and sectioning steps were carried out by our group or by the staff of the Physiology Core of the Yale Core Center for Musculoskeletal Disorders (YCCMD). Selected specimens were decalcified as described [13]. Sections were prepared either by CryoJane or routine paraffin techniques [13]. These were stained by H & E, tartrate-resistant acid phosphatase (TRAP), or alkaline phosphatase (via Sigma kit 86-R or in-house reagents in the YCCMD, using either fast red LB or fast blue BB salt to generate red or blue reaction products, as described [21–23]). Sections from X-gal- and TRAP-stained specimens of control and unloaded MCL insertions from three mice were analyzed histomorphometrically for the numbers of stain-positive cells using the Osteomeasure system software and hardware. Each of these sites at 40X magnification was subdivided into three equal areas that together represented the entire length of the insertion in sagittal view, and the results were expressed as mean ± SE for these nine areas from the three control and three unloaded specimens. The alkaline phosphatase-stained areas from three pairs of legs were quantitated by greyscale analysis in three-four identical rectangular areas per section and expressed as a ratio of unloaded to control values. These data and the semiquantitative unloading responses in cleared specimens were compared by Student's t-test.

RESULTS

Periosteum

As reported previously [13], PTHrP/lacZ expression is confined to the fibrous layer of the periosteum and is not present in the cambial layer in any location or at any age, as shown in Fig. 1A. The β gal activity is not uniform throughout the periosteum, and a particularly high level of activity is seen in the region of the lateral tibial metaphysis and along the anterolateral fibula in a 3-week-old mouse. As anticipated, the PTH1R is found in the subjacent cambial layer (Fig. 1B), confirming paracrine signaling. In different locations and/or at different times, PTHrP-lacZ activity in the fibrous layer of the periosteum seems to be associated with either subjacent osteoclastic activity (Fig. 1C) or subjacent osteoblastic activity (Fig. 1D). The putative relationship of PTHrP expression to periosteal modeling and/or bone accretion in different periosteal sites at different ages is not yet clear and is under study.

Fibrous tendinous and ligamentous insertions

Muscles attach to bone via several categories of entheses [24–27]. These include: a) periosteal muscle insertions, which characterize muscles that attach over a relatively large bone surface

and that comprise a tendinous region that is little more the simple two-layer periosteum, b) fibrous insertions, which typify (frequently major) muscles whose tendons insert at relatively oblique angles into sites that may contain many layers of connective tissue cells as well as fibers that cement them firmly into cortical bone, and c) fibrocartilagenous attachments, which are the most complex and typify the insertions of major muscle groups into an epiphysis (e.g., the gastrocnemius via the Achilles tendon); these comprise both connective tissue and fibrocartilagenous elements that cushion the insertion [24–27]. PTHrP/lacZ is expressed in all of these categories of insertions to one or another extent [13].

Fig. 1E shows the fibrous insertions of the middle collateral ligament (MCL) and semimembraneosus muscle (SM) into the proximal tibial metaphysis at 3 weeks. The MCL itself can be appreciated in this image as the whitish longitudinal band that connects the femoral condyle to the tibial metaphysis. The arrowhead identifies the somewhat egg-shaped SM insertion that begins slightly posterior to the MCL and continues anteriorly underneath it, and the MCL itself inserts slightly inferior the to SM site. Both are intensely β gal-positive. PTH1R expression by ISHH in this region is depicted in a sagittal darkfield image in Fig. 1F; the dark arrow identifies the SM/MCL insertions, the arrowheads the bone collars associated with the secondary ossification center above and the growth plate below, and the white arrow the prehypertrophic chondrocytes in the growth plate. In the MCL/SM site, hybridization is in the distal one-half of the insertion, in the region typically occupied by osteoblasts (see Fig. 1F, Fig. 2D and G, and text below).

Histological and histochemical images of frontal sections of the MCL insertion at 7 weeks are shown in Fig. 2, panels A–D. β gal activity lies at the junction of the MCL and its fibrous insertion (panel 2A) and in panel 2B can be traced from the periosteum above into the insertion site itself, indicating that there is continuity between the fibrous periosteal PTHrP-expressing cells and the PTHrP-expressing fibroblast-like cells in the MCL insertion. This panel (2B) corresponds to the proximal one-half of the attachment and shows the so-called cortical depression into which the MCL inserts and which contains at its base and proximal edge numerous TRAP-positive osteoclasts. The distal one-half of the attachment is devoid of osteoclasts (Fig. 2C) but rather contains an abundance of alkaline phosphatase-positive osteoblasts (Fig. 2D). Some of the indigo β gal reaction product in these MCL images has been lost during the H&E and histochemical staining procedures, but the spatial pattern of β gal activity (i.e., limited to the junction of the MCL and fibrous enthesis) is correctly depicted.

Frontal sections of the SM insertion at 6 weeks are depicted in Fig. 2, panels E–G, stained with H&E, TRAP, and alkaline phosphatase, respectively. In essence, this insertion simply represents a more flamboyant example of the same sorts of images just described, with more widespread β gal activity, a deeper cortical depression, and more TRAP-positive osteoclasts in its proximal one-half and alkaline phosphatase-positive osteoblasts in its distal one-half. The impressiveness of these various activities in this site as compared to the MCL insertion presumably reflects the fact that this is a muscular rather than ligamentous attachment and one associated with a relatively strong hamstring muscle [28]. At the ages depicted in Fig. 2 (6–8 weeks) the mice are actively growing, and both the MCL and the SM should be migrating, which would account for the polarized osteoclastic and osteoblastic activities [29–31]. This question too requires more careful study and will be reported separately.

Mechanical unloading of entheses

The credentials of the PTHrP gene as a mechanically-inducible gene in several cell types have been established for some time [8,32,33]. We used several different protocols to study the potential mechanical inducibility of PTHrP/lacZ in selected entheses.

Tail suspension of rodents is an established technique for inducing hindlimb weightlessness. This method has been used principally to study the effects of unloading on the skeleton [18, 19] and has not to our knowledge been used to study entheses. We focused on 13 mixed-gender PTHrP-lacZ mice at 5–7 weeks of age suspended for 11 days; a like number of sham-suspended PTHrP-lacZ, gender-matched littermates served as controls. We concentrated upon: 1) the fibrous insertion of the adductor magnus into the posteromedial femur [13], 2) the third trochanter on the lateral femur, which bears the fibrous origin of elements of the quadriceps, and 3) the fibrous tibial insertions of the MCL and two hamstrings, the SM and the semitendinosus (ST). We used X-gal-stained and partially-cleared specimens as our primary readout and developed a visual 1–4 graded response scale in which each arbitrary unit corresponded to an estimated 25% reduction in β-gal activity (e.g., a grade 3 score corresponded to a 75% reduction).

Fig. 3, panels A and B, show control and unloaded adductor insertions, respectively, with the latter having a grade 3 response. Nine of 13 (65%) of suspended mixed-gender mice showed a grade 3 or greater response at this site and the remainder a response that was less striking. Fig. 3C shows suspended and control third trochanters (to the left and right, respectively) in which the suspended specimens also showed a grade 3 response. Eight of 13 (60%) of the suspended examples at this site showed a grade 3 or greater response. At the MCL/SM insertions, 10 or 13 (74%) and at the ST insertion 8 of 13 (60%) showed grade 3 or greater responses. The control β gal signals were essentially invariant, so that the experimental variability was entirely a function of responsiveness. While this technique does induce weightlessness, it does not eliminate muscle tone or even a degree of muscle activity at entheses, and ongoing linear growth would be expected in mice at this age. Either or both of these influences might provide residual force input into one or another entheses during these experiments, perhaps accounting for the less dramatic decreases in β gal activity than were associated with the transection experiments, described below. Nevertheless, all of the responses described above were highly significant ($p<.001$).

We next used surgical transection of the tendon/ligament in question immediately proximal to its insertion. With experience, this approach proved to be virtually bloodless, and the entheses themselves were unharmed. Clearly, this method would completely unload an enthesis with respect to either muscle force or the effects of growth. We focused primarily on the MCL/SM and ST sites because of the simplicity of the surgery, sacrificing the mice 7 days after surgery and pooling data from both genders. We used the same graded 1–4 visual scale to score these experiments, as compared to findings in the unoperated, control side.

Fig. 3, panels D and E, show control and transected MCL/SM sites, respectively, the latter with a grade 4 response, in that it was not possible to visually identify the actual insertion site based on β-gal activity in the transected site. A grade 3 or greater response was seen in 13 of 15 (87%) such sites ($p<.001$). Fig. 3, panels F and G, show control and transected ST sites, respectively, the latter again assessed as having a grade 4 response. In this location, we saw a grade 3 or greater response in 11 of 12 (92%) experiments ($p<.001$). The near-complete loss of the βgal signal in unloaded sites was particularly evident in histological sections (panels 3 I and K). In three pairs of control and unloaded sites analyzed by histomorphometry, the mean (± SE) numbers of β gal-positive cells were 432 ± 73 and 2 ± 1 cells/μm^2, respectively. Panels H and I reveal that the near-complete disappearance of PTHrP/lacZ signal on unloading was accompanied by a similar disappearance in alkaline phosphatase activity ($p<.001$), suggesting that the osteoblast population in the trailing edge of the insertion was load-induced and likely driven by PTHrP. An essentially identical pattern was seen at 72 and 96 hours post-transection, so that this response was very rapid (data not shown). Panels J and K show TRAP stains in these same specimens and also revealed a marked reduction ($p<.001$) yet one that was somewhat less dramatic than the alkaline phosphatase response. These findings indicate that

the osteoclastic population at the leading edge of the insertion is also load-induced and may be PTHrP-associated.

Bone cells

We had expected to identify lacZ expression in osteoblasts [34] and perhaps osteoclasts [35] but found no clear β gal activity in these cells in our initial survey [13]. We have now looked at this question more carefully, using the more specific heat-inactivation protocol to score exogenous galactosidase activity [20], looking at an extensive number of sites in the PTHrP-lacZ CD-1 mice, and also after inbreeding the PTHrP-lacZ allele into a C57Bl/6 background. The proximal tibial growth plate, secondary ossification center, and metaphysis are prime locations in which to identify osteoblasts during rapid growth, yet we could identify no β gal activity in any of these sites (Fig. 4). For example, Fig. 4A and C reveal β gal-positive subarticular and proliferative chondrocyte populations, but there is no such activity in the alkaline phosphatase-positive populations depicted in panel B, which included osteoblasts in the primary spongiosa, secondary ossification center, and grove of Ranvier in the bone collar (arrows). We have looked at the proximal tibia also in a C57Bl/6 background and find β gal activity only in chondrocytes (Fig. 1D). Similarly, in the CD-1 PTHrP-lacZ mouse population, we found no β-gal activity in periosteal osteoblasts, endosteal osteoblasts, bone-lining cells, or calvarial osteoblasts (data not shown).

Thus, in the PTHrP-lacZ mouse, PTHrP/lacZ expression is confined to chondrocytes and to connective tissue cells in the periosteum and insertion sites and cannot be detected in bone cells themselves. Further, all of these PTHrP-expressing cells and structures are at the periphery of endochondral bones and correspond to elements at which bones interact or are attached to each other and/or to the surrounding musculature.

DISCUSSION

It is by no means clear why the experiences of different groups vary as regards the presence or absence of PTHrP expression in bone cells, osteoblasts in particular. Our experience with immunohistochemistry using various region-specific anti-PTHrP antisera in different tissues has lead us to doubt that this technique is capable of reliably detecting the very low levels of PTHrP in most sites, and the marked variability of IH findings reported in the literature reinforces this concern [reviewed in 13]. A technical explanation as to why we might somehow miss lacZ expression in osteoblasts also seems unlikely, as expression is being driven in this instance by the endogenous PTHrP gene controlling region itself, and lacZ has been frequently used to score gene expression in osteoblasts by exogenous promoters or as a readout of Cre targeting in R26R mice [36 and references therein]. We also estimate that the PTHrP-lacZ mouse provides an approximately 5-fold or more increase in detection sensitivity as compared to conventional immunohistochemical and in situ hybridization techniques, which is very similar to the figure reported previously by a group that used the same strategy to score a low-abundance gene product (13,37). However, there are also functional data implicating PTHrP as a anabolic osteoblastic product in inbred C57BL/6 mice [34], although inbreeding the PTHrP-lacZ allele into this background did not alter our results. At present, we are simply unable to account for these different findings and interpretations.

Taken together, our data suggest that in long bones a major site of PTHrP gene expression is in the connective tissues that envelope these bones and connect them to each other and to the surrounding musculature. Another example of this phenomenon is the expression of PTHrP/lacZ in the perichondrium of the costal cartilage [7,9,13]. These surrounding mesenchymal/connective tissue structures arise from precursors present in the early limb buds and can be detected by the presence of the scleraxis gene from this stage through the life of the mouse (38). Many of these connective tissue structures express PTHrP at the junctions of the skeletal

elements with each other and with the musculature, essentially inviting the hypothesis that the gene might be regulated by mechanical force in these sites.

PTHrP has been known to be a mechanically-induced gene since the early 1990s. This induction has been demonstrated in essentially every smooth muscle structure in the body, in which PTHrP is induced by distention and serves to relax the smooth muscle structure in question, allowing it to accommodate pressure or gradual filling [8]. More recently, mechanotransduction of PTHrP has been demonstrated in cultured chondrocytes and bone-derived mesenchymal cells, which is a relevant point here as evidence that PTHrP is mechanically-stimulated in a cell-autonomous fashion rather than as a consequence of (or in addition to) being driven by signals relayed from the neuron-like osteocytic network in cortical bone [39]. We used two different techniques to demonstrate the load-dependence of PTHrP expression in selected insertions, and these were useful when used as a pair, as they targeted different entheses. Of these, tail suspension seemed to be less predictable as well as less complete as an unloading method, likely due to some degree of residual input of tension as a consequence of muscle tone and/or growth. Transection was almost uniformly effective and seemed to produce near-complete functional unloading. Certainly, taken together, these findings indicate that mechanotransduction has a major influence on PTHrP expression in both ligamentous and tendinous insertion sites and imply that the function(s) of PTHrP in these locations may be associated with responses to mechanical force.

It is evident that PTHrP expression in the periosteum and entheses is at least logistically associated with subjacent active bone cell populations, although it is not clear whether this association is primarily with osteoblasts, osteoclasts, or both. Our results from ISHH for PTH1R are compatible with primarily PTH1P-expressing osteoblastic receptor-based populations in some of these sites, and the striking correlation between the disappearance of the β gal and alkaline phosphatase activity in the unloaded MCL/SM entheses is certainly compatible with load and PTHrP induction of the osteoblasts in these sites. It is clear from the enormous literature on the so-called anabolic and catabolic effects of PTH and PTHrP in vivo that PTH and PTHrP are capable of regulating the formation and/or activities of osteoblasts and/or osteoclasts. However, it also has been shown that in the microenvironment of the tooth during its eruption phase PTHrP drives completely uncoupled osteoclastic bone resorption via the mediation of mesenchymal PTH1R-bearing cells rather than osteoblasts [40]. Thus, at present, the most appropriate interpretation would appear to be that PTHrP may be able to drive either osteoblastic or osteoclastic activity/recruitment, or both, and that the seeming enigma of PTHrP function at bone surfaces might prove to have as its basis similar biological mechanisms to those that underlie the anabolic and catabolic activities of the PTH/PTHrP peptides in the general skeleton.

As regards function(s), our findings are compatible with several interpretations, none of which represents more than a working hypothesis at present. In entheses, PTHrP could drive the underlying osteoblastic activity that ultimately anchors the insertion in question into first woven and subsequently lamellar cortical bone [26,28]; conversely, PTHrP could drive osteoclastic activity that prevents such insertions from becoming so cemented that they loose compliance and all capacity to cushion the mechanical forces that they transmit. In addition, it is known that entheses that insert into a metaphysis must migrate as the bone grows from the epiphyseal growth plate, lest the insertion wind up as a few functionless shreds that insert into the mid-diaphysis [29,31–33]. This migration is associated with the kinds of polarized osteoclastic and osteoblastic activities we describe here, and driving such migration would be an appealing function for a mechanically-induced regulatory gene. This question is presently under study. Finally, the strong β gal activity in the metaphyseal periosteum in young mice suggests that PTHrP in this location might be associated with the modeling of this structure that accompanies linear growth, and the pronounced β gal signal in the perichondrium/

periosteum flanking the primary ossification center (Fig. 4F) suggests that Indian hedgehog might induce the bone collar in this location via the mediation of PTHrP (9). These questions too are under study.

ACKNOWLEDGEMENTS

Nancy Troiano and Chris Coady in the Physiology Core of the Yale Center for Musculoskeletal Disorders (YCCMD) provided expertise in histology and histochemistry; Barbara Dreyer provided assistance at many levels, and J.P. Zhang provided early assistance with in situ hybridization histochemistry. We thank Ann DeCosta for attention to detail in preparing the manuscript.

Supported in part by NIH grants DK62515, DK48108, DK075626, AR46032 (YCCMD), and DK45735 (DERC).

REFERENCES

1. Philbrick WM, Wysolmerski JJ, Galbraith S, Orloff JJ, Yang KH, Vasavada RC, Weir EC, Broadus AE, Stewart AF. Defining the roles of parathyroid hormone-related protein in normal physiology. Physiol Rev 1996;76:127–173. [PubMed: 8592727]
2. Strewler GJ. The physiology of parathyroid hormone-related protein. N Engl J Med 2000;342:177–185. [PubMed: 10639544]
3. Martin TJ. Properties of parathyroid hormone-related protein and its role in malignant hypercalcemia. Qual J Med 1990;76:771–786.
4. Jüppner H, Abou-Samra A-B, Freeman M, Kong XF, Schipani E, Richards J, Kolakowsik LF, Hock J, Potts JT, Kronenberg HM, Segre GV. A G protein-linked receptor for parathyroid hormone and parathyroid hormone-related peptide. Science 1991;254:1024–1026. [PubMed: 1658941]
5. Nissenson, RA. Receptors for the parathyroid hormone and parathyroid hormone-related protein signaling and regulation. In: Bilezikian, JP., editor. The Parathyroids. 2nd ed.. New York, NY: Acad Press; 2001. p. 93-104.
6. Wysolmerski, JJ.; Stewart, AF.; Martin, JT. Physiologic actions of PTH and PTHrP: V. Epidermal, mammary reproductive, and pancreatic tissue. In: Bilezikian, JP., editor. The Parathyroids. 2nd ed.. New York, NY: Acad Press; 2001. p. 275-292.
7. Karaplis AC, Luz A, Glowacki J, Bronson RJ, Tybolewicz VLJ, Kronenberg H, Mulligan RC. Lethal skeletal dysplasis from targeted disruption of the parathyroid hormone-related peptide gene. Genes & Dev 1994;8:277–289. [PubMed: 8314082]
8. Clemens, TL.; Broadus, AE. Physiologic actions of PTH and PTHrP: IV. Vascular, cardiovascular, and neurologic actions. In: Bilezikian, JP., editor. The Parathyroids. 2nd ed.. New York, NY: Acad Press; 2001. p. 261-274.
9. Kronenberg HM. Developmental regulation of the growth plate. Nature 2003;423:332–336. [PubMed: 12748651]
10. Lee K, Deeds JD, Segre GV. Expression of parathyroid hormone-related peptide and its receptor messenger ribonucleic acids during fetal development of rats. Endocrinology 1995;136:453–463. [PubMed: 7835276]
11. Holt EH, Lu C, Dreyer BE, Dannies PS, Broadus AE. Regulation of parathyroid hormone-related peptide gene expression by estrogen in GH4C1 rat pituitary cells has the pattern of a primary response gene. J Neurochem 1994;62:1239–1246. [PubMed: 8133258]
12. Ikeda K, Mangin M, Dreyer BE, Webb AC, Posillico JT, Stewart AF, Bander NH, Weir EC, Insogna KL, Broadus AE. Identification of transcripts encoding a parathyroid hormone-like peptide in messenger RNAs from a variety of human and animal tumors associated with humoral hypercalcemia of malignancy. J Clin Invest 1988;81:2010–2014. [PubMed: 2454953]
13. Chen X, Macica CM, Dreyer BE, Hammond VE, Hens JR, Philbrick WM, Broadus AE. Initial characterization of PTH-related protein gene-driven lacZ expression in the mouse. J Bone Miner Res 2006;21:113–123. [PubMed: 16355280]
14. Hofmann A, Nolan GP, Blau HM. Rapid retrovial delivery of tetracycline-inducible gene in a single autoregulatory cassette. Proc Natl Acad Sci USA 1996;93:5185–5190. [PubMed: 8643550]

15. Margolis TP, Bloom C, Dobson AT, Feldman LT, Stevens JG. Decreased reporter gene expression during latent infection with HSV LAT promoter construct. Virology 1993;197:585–592. [PubMed: 8249281]
16. Jacobsen KD, Willumsen BM. Kinetics of expression of inducible β-galactosidase in murine fibroblasts: high initial rate compared to steady-state expression. J Mol Biol 1995;252:289–295. [PubMed: 7563050]
17. Johnson RB. The bearable lightness of being: Bones, muscles, and spaceflight. Anat Rec (New Anat) 1998;253:24–27.
18. Morey-Holton ER, Globus RK. Hindlimb unloading rodent model: technical aspects. J Appl Physiol 2002;92:1367–1377. [PubMed: 11895999]
19. Squire M, Donahue L-R, Rubin C, Judex S. Genetic variations that regulate bone morphology in the male mouse skeleton do not define its susceptibility to mechanical unloading. Bone 2004;35:1353–1360. [PubMed: 15589216]
20. Young DC, Kinsley SD, Ryan KA, Dutko FJ. Selective inactivation of eukaryotic β-galactosidase in assays for inhibitors of HIV-1 TAT using bacterial β-galactosidase as a reporter enzyme. Anal Biochem 1993;215:24039.
21. Kacena MA, Troiano NW, Wilson KM, Coady CE, Horowitz MC. Evaluation of two different methylmethacrylate processing, infiltration and embedding techniques on the histological, histochemical and immunohistochemical analysis of murine bone specimens. J Histotechnol 2004;27:119–130.
22. Wysolmerski JJ, Philbrick WM, Dunbar ME, Lanske B, Kronenberg H, Karaplis AC, Broadus AE. Rescue of the parathyroid hormone-related protein knockout mouse demonstrates that parathyroid hormone-related protein is essential for mammary gland development. Development 1998;125:1285–1294. [PubMed: 9477327]
23. Philbrick WM, Dreyer BE, Nakchbandi IA, Karaplis AC. Parathyroid hormone-related protein is required for tooth eruption. Proc Natl Acad Sci USA 1998;95:11846–11851. [PubMed: 9751753]
24. Benjamin M, Kumai T, Milz S, Boszczyk BM, Boszczyk AA, Ralphs JR. The skeletal attachment of tendons – tendon 'entheses'. Comp Biochem Physiol Part A 2002;133:931–945.
25. Doschak MR, Zernicke RF. Structure, function and adaptation of bone-tendon and bone-ligament complexes. J Musculoskeletal Neuronal Interact 1997;5:35–40.
26. Benjamin M, Ralphs JR. Tendons and ligaments – an overview. Histol Histopathol 1997;12:1135–1144. [PubMed: 9302572]
27. Matyas JR, Bodie D, Andersen M, Frank CB. The developmental morphology of a "periosteal" ligament insertion: growth and maturation of the tibial insertion of the rabbit medial collateral ligament. J Orthopaedic Res 1990;8:412–424.
28. Burr DB. Muscle strength, bone mass, and age-related bone loss. J Bone Min Res 1997;12:1547–1540.
29. Wei X, Messner K. The postnatal development of the insertion of the medial collateral ligament in the rat knee. Anat Embryol 1996;193:53–59. [PubMed: 8838496]
30. Dörfl J. Migration of tendinous insertions. I. Cause and mechanism. J Anat 1980;131:179–195. [PubMed: 7440401]
31. Dörfl J. Migration of tendinous insertions. II. Experimental modifications. J Anat 1980;131:229–237. [PubMed: 7462092]
32. Tanaka N, Ohno S, Honda K, Tanimoto K, Doi T, Ohno-Nakahara M, Tafolla E, Kapila S, Tanne K. Cyclic mechanical strain regulates the PTHrP expression in cultured chondrocytes via activation of the Ca^{2+} channel. J Dent Res 2005;84:64–68. [PubMed: 15615878]
33. Chen X, Macica CM, Ng KW, Broadus AE. Stretch-induced PTH-related protein gene expression in osteoblasts. J Bone Min Res 2005;20:1454–1461.
34. Miao D, He B, Jiang Y, Kobayashi T, Soroceanu MA, Zhao J, Su J, Tong X, Amizuka N, Gupta A, Genant HK, Kronenberg HM, Goltzman D, Karaplis AC. Osteoblast-derived PTHrP is a potent endogenous bone anabolic agent that modifies the therapeutic efficacy of administered PTH 1–34. J Clin Invest 2005;115:2402–2411. [PubMed: 16138191]

35. Kartsogiannis V, Moseley J, McKelvie B, Chou ST, Hards DK, Ng KW, Martin TJ, Zhou H. Temporal expression of PTHrP during endochondral bone formation in mouse and intramembranous bone formation in an in vivo rabbit model. Bone 1997;21:385–392. [PubMed: 9356731]

36. Dacquin R, Starbuck M, Schinke T, Karsenty G. Mouse α1(I)-collagen promoter is the best known promoter to drive efficient Cre recombinase expression in osteoblast. Dev Dynamics 2002;224:245–251.

37. Mountford P, Zevnik B, Düwel AN, Nickols J, Ji M, Dani C, Robertson M, Chambers I, Smith A. Dicistronic targeting constructs: reporters and modifiers of mammalian gene expression. Proc Natl Acad Sci USA 1994;91:4303–4307. [PubMed: 8183905]

38. Pryce BA, Brent AE, Murchison MD, Tabin CJ, Schweitzer R. Generation of transgenic tendon reposrts, ScxGFP and ScxAP, using regulatory elements of the scleraxis gene. Dev Dyn 2007;236:1677–1682. [PubMed: 17497702]

39. Turner CH, Robling AG, Duncan RL, Burr DB. Does bone behave like a neuronal network? Calcif Tissue Internatl 2002;70:435–442.

40. Philbrick WM, Dreyer BE, Nakchbandi IA, Karaplis AC. Parathyroid hormone-related protein is required for tooth eruption. Proc Natl Acad Sci USA 1998;95:11846–11851. [PubMed: 9751753]

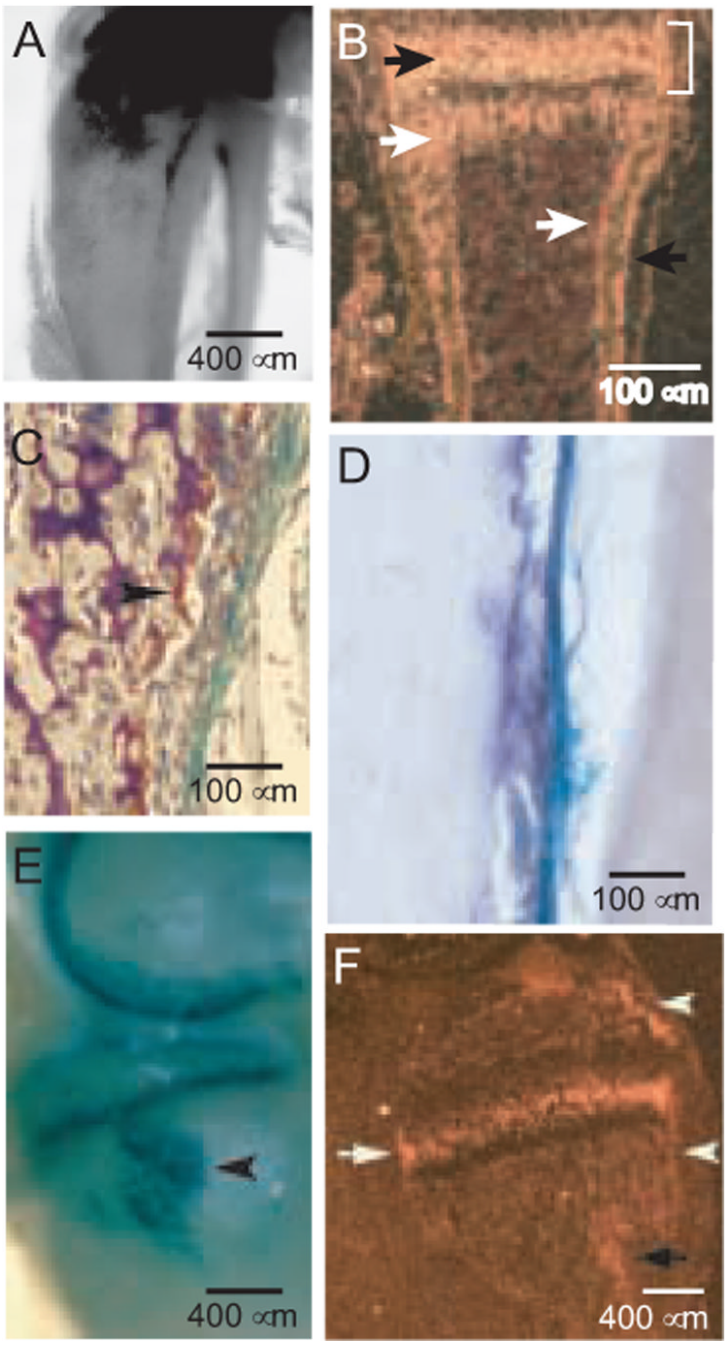

FIG. 1. Images of the periosteum and the medial collateral ligament and semimembraneosus insertions

(A) β gal-activity in the proximal tibia and fibula in a cleared specimen at 3 weeks (40X). The intense activity in the most proximal regions is cartilaginous, as reported previously [13]. (B) PTH1R localization by ISHH in a wild-type metacarpal at 7 days. The prehypertrophic chondrocytes of the growth plate (black arrow), osteoblasts in the metaphysis and endosteum (white arrows), periosteal osteoblasts (black arrow), and bone collar (bracket) are indicated. Note that the osteoblasts in the bone collar and periosteum form a continuum, as do the osteoblasts in the primary spongiosa and endosteum. (C) β gal and TRAP activities in the metaphyseal region of the proximal tibia at 6 weeks (200X). The arrowhead identifies an

osteoclast. (D) Alkaline phosphatase stain of the medial surface of the tibia distal to the MCL insertion at 7 weeks (200X). Some of the β gal stain in the fibrous layer remains, and the somewhat pleiomorphic alkaline phosphatase-positive osteoblasts lie beneath on an irregular periosteal surface. (E) X-gal-stained medial aspect of a cleared distal femur and proximal tibia in a PTHrP-lacZ mouse at 3 weeks of age. The intense semicircular β gal signals in the distal femur and proximal tibia are cartilage-associated (40X image). The arrowhead identifies the SM insertion at the superior margin of the MCL insertion. (F) PTH1R mRNA expression by ISHH in a sagittal section of the medial side of the proximal tibia at 3 weeks, wild-type mouse. The black arrow identifies the MCL/SM insertions, the arrowheads the bone collar associated with the secondary ossification center above and the growth plate below (the latter sometimes referred to as the ring of Lacroix), and the white arrow the intense signal associated with prehypertrophic chondrocytes in the growth plate. Darkfield image (40X).

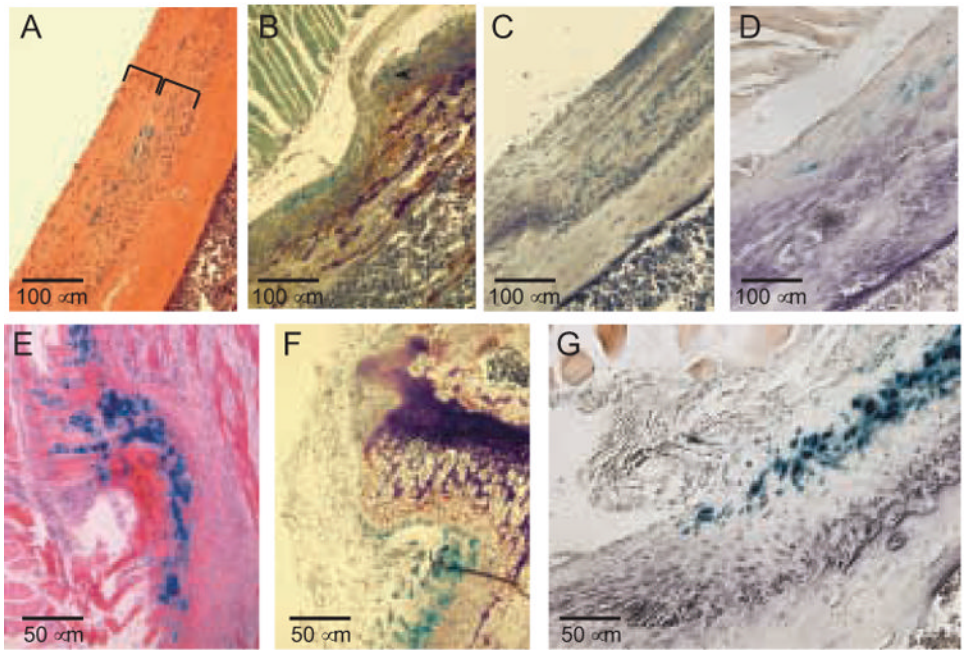

FIG. 2. Histological structure of the MCL and SM insertions

(A) X-gal-and H&E-stained frontal section of the MCL insertion at 7 weeks. The width of the MCL itself is defined by a bracket, as is the subjacent insertion site. Note that β gal activity is confined to the actual junction of the MCL and the underlying connective tissue that lies in the cortical depression, the latter comprising the remainder of the entheses. (B) X-gal- and TRAP-stained proximal one-half of the MCL insertion at 7 weeks. Note that the β gal signal in the periosteum that underlies the unattached portion of the MCL is continuous with the layer of β gal-positive fibroblast-like cells in the MCL insertion. Note also that the TRAP-positive osteoclasts are concentrated proximally. (C) TRAP/X-gal stains of the distal one-half of the MCL insertion shown in B; note there are no osteoclasts. (D) X-gal-and alkaline phosphatase-stained distal one-half of an MCL insertion at 4 weeks. The purple alkaline phosphatase product is both cellular and extracellular. All four panels (A–D) are 200X. (E–G) X-gal-stained images of a frontal section of the SM insertion. The counterstains are H&E (D, 400X), TRAP (E, 400X), and alkaline phosphatase (F, 400X).

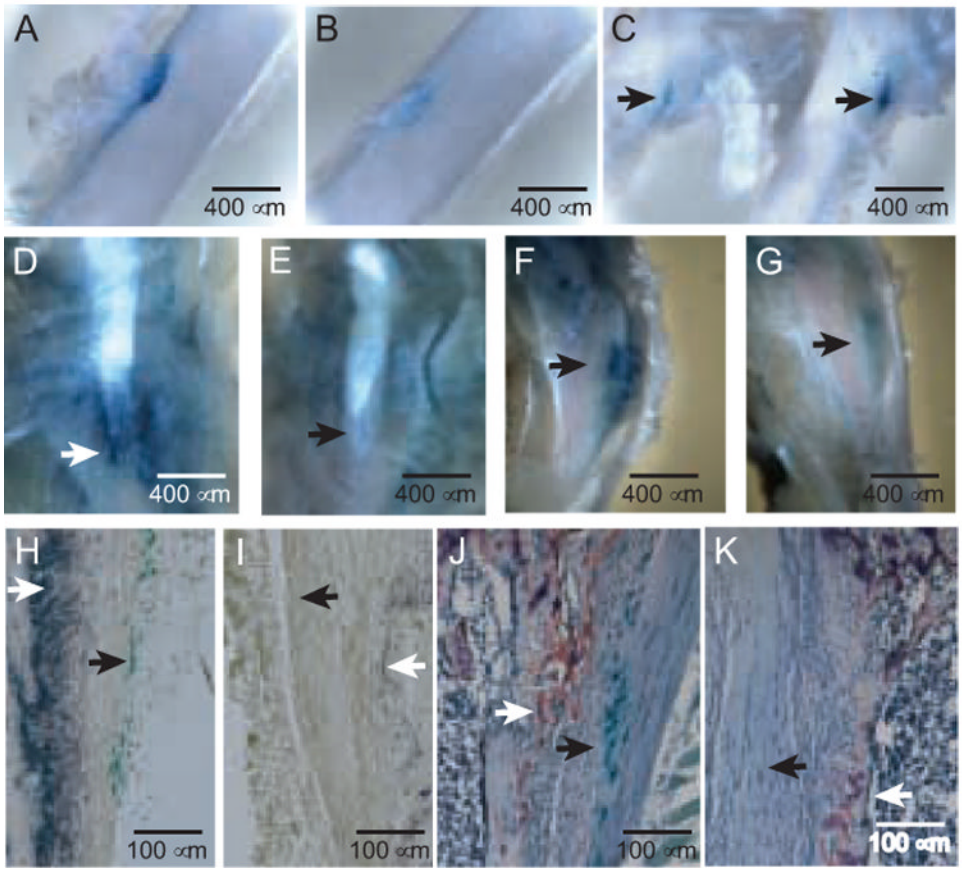

FIG. 3. Unloading of fibrous-bony insertion sites by tail suspension (A–C) or surgical transection (D–K)

(A and B) Sham control (A) and suspended (B) insertions of the adductor magnus into the mid-posterior femur in a 7-week-old male PTHrP-lacZ mouse suspended for 11 days, cleared images of X-gal-stained specimens (50X). (C) Origin of the vastus lateralis (arrows) from the third trochanter of a 7-week-old mouse suspended (image to left) or shamed (to right) for 7 days. (D and E) Control (D) and transected (E) MCL/SM insertions (arrows) in a 4-week-old PTHrP-lacZ mouse sacrificed 7 days following transection, 40X. (F and G) Control (F) and transected (G) semitendinosus insertions (arrows) in a 4-week-old mouse sacrificed 7 days following transection, 40X. (H and I) Control (H) and transected (I) MCL insertions in the left and right legs, respectively, of a 5-week-old PTHrP-lacZ mouse 7 days after surgery, X-gal and alkaline phosphatase stains. The closed arrow identifies β gal-positive cells and the open arrow alkaline-phosphatase activity. The images focus on the trailing edge of the insertion. The ratio of unloaded: control integrated greyscale values for the alkaline phosphatase-stained areas was 0.25 ± 0.03 (mean ± SE, $p<0.001$). (J and K) Control (J) and transected (K) MCL insertions contiguous to those shown in panels H and I, X-gal and TRAP stains. The closed and open arrows identify β gal- and TRAP-positive cells, respectively. The images focus on the leading edge of the MCL, flanked internally by the trabecular bone of the tibial metaphysis. The mean (± SE) numbers of TRAP-positive cells fell from 114 ± 23 in the control to 22 ± 8 cells/μm² in the transected sites ($p<0.001$).

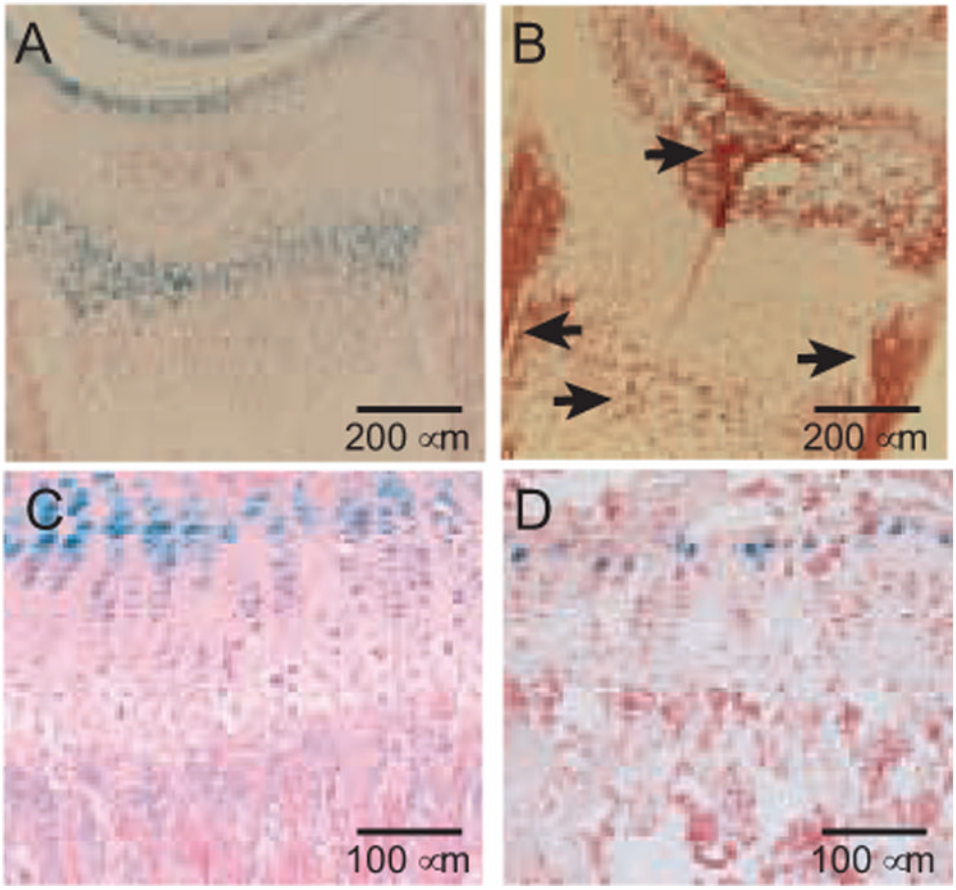

FIG. 4. Osteoblast populations in the PTHrP-lacZ mouse do not contain β gal activity

(A and B) CryoJane sections of day 12 (D12) proximal tibia stained with X-gal and counterstained with nuclear fast red (A, 100X) or with alkaline phosphatase (B, 100X) using a fast red violet LB salt that generates a red reaction product. The arrows in B identify the secondary ossification center, primary spongiosa, groove of Ranvier, and the bone collar, which is seen as a vertical strip of cells with a very high activity. It should be noted that hypertrophic chondrocytes also produce alkaline phosphatase, as seen in the population in the secondary ossification center just subjacent to the articular chondrocytes. (C) Proximal tibia at 6 weeks, X-gal-stained and counterstained with H & E (200X). (D) CryoJane section from 8-week-old PTHrP-lacZ mouse on a C57BL/6 background, stained and counterstained as in A. There is no β gal activity in the primary spongiosa in either panel C or D.